



# Proteinous Polymeric Shell Decorated Nanocrystals for the Recognition of Immunoglobulin M

Sibel Büyüktiryaki<sup>1</sup> · Filiz Yılmaz<sup>2</sup> · Rıdvan Say<sup>3,4</sup> · Arzu Ersöz<sup>2,4,5</sup>

Received: 26 November 2018 / Accepted: 25 March 2019 / Published online: 8 April 2019  
© Springer Science+Business Media, LLC, part of Springer Nature 2019

## Abstract

This study demonstrates the preparation of photosensitively orientated and crosslinked proteinous polymeric shell having quantum dot based nanocrystals through Amino acid Decorated and Light Underpinning Conjugation Approach (ANADOLUCA). ANADOLUCA is based on photo-electron transfer method and uses these decorated nanocrystals for specifically and effectively recognition and detection of Immunoglobulin M in the aqueous environment. The conjugation method effectively provides an orientation of affinity pairs on the surface of quantum dots nanocrystals. This photosensitive ruthenium-based amino acid monomer is a synthetic and inexpensive material for the preparation of bioconjugates. The nanocrystals give advantages for using a wide pH and temperature range. The construction and preparation method is applicable to silica materials, superparamagnetic particles, quantum dots, carbon nanotubes, Ag/Au nanoparticles, Au surfaces, and polymeric materials. This prepared proteinous polymeric shell decorated nanocrystals are of great potential in applications in life sciences and can be used in infection case studies or allergy symptoms.

**Keywords** Orientated conjugation · Recognition of IgM · ANADOLUCA method · Quantum dots · Photosensitive crosslinking

## Introduction

Immunoglobulin M (IgM) antibodies are the highest antibody with the molecular weight of approximately 950 kDa [1]. Mostly found as a pentamer but also it can be found as a hexamer. Since each IgM monomer contains two antigen binding sites, a pentameric IgM has ten binding sites [2, 3]. IgM antibodies are about 5% to 10% of all the antibodies in the body. The average concentration of IgM is  $1.5 \text{ mgmL}^{-1}$  in the normal human serum [4]. IgM antibodies are found in blood and lymph fluid and are the first type of antibodies formed

during the primary immune response for fighting infection by B cells. The amount of IgM is increased in the early days of infection. Then the amount of IgM decreases, while the amount of immunoglobulin G (IgG) increases. A high ratio of IgM states the early stage of infection. Pentameric structure of IgM allows rapid clearing of blood from antigens during the primary stages of an infection. Detection of a recent or ongoing infection can be achieved with the sensing of specific IgM antibodies [5–7]. Determination of IgM has been performed in many studies to determine chronic hepatitis [8], rubella virus [9], dengue virus [10–12], measles virus [13], typhoid, rheumatoid arthritis, cirrhosis, malaria, Waldeström macroglobulinemia and malign plasma cell tumors [14]. Therefore sensitive recognition and determination of IgM are substantial for clinical studies. As a totally different from other serum immunoglobulins, human IgM contains a high amount of mannose [7, 15]. Because of this, Concanavalin A (Con A) which act as a mannose binder [16, 17] have been used for the recognition of IgM. Con A is widely used in the characterization of glycoproteins, purification of macromolecules in lectin affinity chromatography [17, 18] and diagnosis of diseases in the existence of specific sugars like mannose [19].

In recent years, nanomaterials like silver nanoparticles, gold nanoparticles, carbon nanotubes, magnetic nanoparticles,

✉ Arzu Ersöz  
arzuersoz@eskisehir.edu.tr

<sup>1</sup> Yunusemre Vocational School, Anadolu University, Eskisehir, Turkey

<sup>2</sup> Department of Chemistry, Eskişehir Technical University, Eskişehir, Turkey

<sup>3</sup> Department of Chemistry, Anadolu University, Eskişehir, Turkey

<sup>4</sup> Bionkit Co Ltd., Anadolu University Teknopark, Eskişehir, Turkey

<sup>5</sup> Fen Fakültesi, Kimya Bölümü, Eskişehir Teknik Üniversitesi, Yunus Emre Kampüsü, 26470 Eskişehir, Turkey

silica nanoparticles and quantum dots (QDs) are of great interest for researchers. Nanomaterials improve the performance of biosensors, enhance the binding points, the sensitivity and the selectivity, reduce the detection time and push the detection limit due to having large surface area [20]. QDs are fluorescent semiconductor nanoparticles which have advantages because of broad excitation spectra, adjustable and narrow emission spectra by depending on size. They are highly luminescent, long luminescence lifetime and stable against photobleaching [21]. QDs have advantages labeling nucleic acids or proteins for optical detection compared to organic fluorophores. Since water-soluble QDs enhance stability and biocompatibility of QDs, water-soluble QDs have widely used for biological and medical applications [22]. The functionalization and oriented conjugation of biomolecules to QD surface are one of the most important factors, since biomolecules should not lose natural binding activity. The conjugation of the biomolecules must be in the appropriate direction to achieve an effective binding activity. Biomolecules immobilization on the QD surface can be done with covalent or non-covalent binding [23]. Covalent immobilization provides highly surface covering, an irreversible, stable, reproducible and orientated immobilization [23, 24].

An Aminoacid Decorated and Light Underpinning Conjugation Approach (ANADOLUCA) which contains photosensitive bis pyridyl ruthenium (II) ion ( $[\text{Ru}(\text{bipyridyl})_2]^{2+}$ ) and amino acid based functional monomer such as methacryloylamido tyrosine (MATyr) monomers was developed for covalent crosslinking of biomolecules. This simple and inexpensive conjugation method effectively provides orientated crosslinking of proteins on the nanoparticle surface. Prepared lectin and an antibody having cross-linked nanocrystals have advantages for using at wide pH and temperature range, without any distortion in their structure and activities [25, 26]. It also provides a way to increase the QDs stability of nanocrystals with polymeric shells.

The nanocrystals consist of Con A and anti-IgM were effectively photoimmobilized on the surface of QDs in one step in the presence of chlorobis(2–2-bipyridyl)-methacryloylamidotyrosine-Ruthenium(II) (MATyr-Ru(bipyridyl)<sub>2</sub>Cl), ammonium persulfate (APS) and daylight. Photosensitive Ru (II) based functional monomer (MATyr-Ru(bipyridyl)<sub>2</sub>Cl) was synthesized and then characterized by using nuclear magnetic resonance spectrometry (NMR) and matrix-assisted laser desorption ionization time of flight mass spectrometry (MALDI-TOF MS). Functionalization of QD was performed with methacryloylamido cysteine (MACys) and methacryloylamidotyrosine (MATyr) monomers. After this functionalization, immobilization and crosslinking of Con A and anti-IgM on QDs were performed in the presence of photosensitive Ru (II) based functional monomer in daylight. The interactions between nanocrystals having proteinous shell and IgM were studied using fluorescence spectrophotometer at

different IgM concentrations. The binding affinity of each QD based nanocrystals was investigated for the recognition of IgM by taking advantage of QDs fluorescent properties. Affinity constants for Con A and anti-IgM conjugated QDs were found to be  $42.75 \times 10^9 \text{ M}^{-1}$  and  $32.1 \times 10^9 \text{ M}^{-1}$ , respectively. The usage of ANADOLUCA method as a cross-linking and conjugation of the affinity proteins for the decoration of QDs was provided for the effective recognition of IgM in aqueous environments.

## Material and Methods

### Materials and Instruments

Benzotriazole, Methacrylic Acid, Triethylamine, L-Tyrosine, trifluoroacetic acid (TFA), acetonitrile (MeCN) and L-Cysteine were provided by Sigma-Aldrich (St. Louis, MO, USA). For the purification of water, Barnstead NANO pure ultrapure water system was used. Vario ELIII elemental analyzer was used for the elemental analyses. Nuclear magnetic resonance spectrometry (NMR) characterizations of the synthesized functional monomers were performed by using 500 MHz Bruker Ultra-shield NMR. All matrix-assisted laser desorption ionization time of flight mass spectrometry (MALDI-TOF MS) analyses were performed by Voyager Biospectrometry STR Workstation. The following procedure was applied for the MALDI-TOF MS analyses: The applied acceleration voltage and delay time were 20 kV and 100 ns, respectively. The positive reflector and delayed extraction modes were used for mass analysis. 1  $\mu\text{L}$  of sample solution was mixed with 24  $\mu\text{L}$  of a  $10 \text{ mg mL}^{-1}$  of  $\alpha$ -cyano-4-hydroxycinnamic acid (CHCA, as a matrix) solution in MeCN/0.2% TFA. 1  $\mu\text{L}$  of this mixture was spotted onto a MALDI-TOF MS sample plate and waited to dry for a while. Then, MALDI-TOF MS spectra were obtained. A Carry Eclipse Varian Fluorescence Spectrophotometer as used for the photo-luminescence analyses.

### Synthesis of Aminoacid Based Monomer and Ruthenium Based Functional Co-Monomer

For this purpose, the methacryloylamido tyrosine (MATyr) monomer and methacryloylamido cysteine (MACys) were synthesized applying previously published procedure [25, 27].

Dichloro bis pyridyl ruthenium (II) ( $\text{RuCl}_2(\text{bipyridyl})_2$ ) and ruthenium based functional co-monomer (MATyr-Ru(bipyridyl)<sub>2</sub>Cl) were synthesized by using the reported procedure [25, 26]. The monomer characterization was carried out by MALDI-TOF MS and NMR. After then photosensitive ruthenium-based functional monomer was interacted with

guanine and polymerized with APS in daylight. Oligomer characterization was carried out by MALDI-TOF MS.

### Synthesis of Quantum Dots

A previously reported procedure was applied for the synthesis of quantum dots (QDs) [25, 28]. For this purpose, 20 mL of 0.01 M Cd(CH<sub>3</sub>COO)<sub>2</sub>·2H<sub>2</sub>O solution was prepared in EtOH. Then, it was allowed to stir for 20 min at N<sub>2</sub> atmosphere. 20 mL of 0.01 M Na<sub>2</sub>S was then slowly added to this solution and allowed to stir at N<sub>2</sub> atmosphere for 20 min. Finally, the precipitated QDs were centrifuged at 14000 rpm for 15 min, washed with deionized H<sub>2</sub>O and allowed to dry at room temperature.

### Functionalization of Quantum Dots with Amino Acid Based Monomers

The synthesized QDs were functionalized with MACys and MATyr monomers, separately. In the first step of the functionalization process, 5 mL of QDs were dispersed in EtOH. Then, 10 mL of MACys (0.018 M) was added into this mixture for conjugation of the methacryloyl groups of the monomer on the surface of QDs. Functionalized QDs were washed four times with EtOH and deionized H<sub>2</sub>O for the removal of unreacted -SH groups. At the end of this process, a layer of MACys was successfully formed on the surface of the QDs. The prepared QDs functionalized with MACys were then washed EtOH and deionized H<sub>2</sub>O for four times for the removal of unreacted functional monomers. After MACys functionalization, fluorescence measurement was performed by diluting 20 times. Then, MACys functionalized QDs was mixed with MATyr solution throughout the day (5 mg monomer in 20 mL EtOH) and finally functionalized QDs were then washed EtOH and deionized H<sub>2</sub>O for four times for the removal of unreacted functional monomers.

### The Decoration of Concanavalin a and Anti-Immunoglobulin M Functionalized Quantum Dots and Interaction with Immunoglobulin M

Firstly, 5 ppm 1 mL of Con A solution, 100 μL of photosensitive ruthenium-based amino acid oligomer and 100 μL of 100 mM APS in phosphate buffer pH 7.4 were added into 2 mL of MACys and MATyr, separately, modified QDs solution and polymerized in daylight throughout the day. Then, Con A conjugated QDs were centrifuged and dispersed to 2 mL with phosphate buffer. And then, these particles were separated into five parts and each part interacted with five different concentrations of IgM solutions (10<sup>-2</sup> ppm–1 ppm). The fluorescence intensity values of these interactions were measured by 20

times dilution as was done above synthesis. Anti IgM conjugated QDs were prepared applying the same procedure and interacted with IgM solutions. IgM desorption was performed with 0.1 M NaCl solution.

## Results and Discussion

### Characterization Studies of Amino Acid and Ruthenium-Based Monomers

The characterization of the synthesized functional monomers MATyr, MACys and photosensitive ruthenium based functional monomer (chlorobis(2–2-bipyridyl)-methacrylamidotyrosine-Ruthenium(II); MATyr-Ru(bipy)<sub>2</sub>Cl) was carried out by using NMR and MALDI-TOF MS. The obtained data from these experiments are in the following:

<sup>1</sup>H NMR data for MACys monomer were given the following: <sup>1</sup>H (500 MHz, DMSO-d<sub>6</sub> and D<sub>2</sub>O): δ: In DMSO-d<sub>6</sub> two single peaks between 7.7–7.4 ppm were observed and because these peaks were lost in D<sub>2</sub>O, it is supposed that these are –SH and –NH peaks. The peaks at 5.7 ppm (s, 1H) and 5.3 ppm (s, 1H), 4.2 ppm (m, 1H), 3.1–3.0 ppm (m, 2H) and 1.9 ppm (s, 3H) were assigned to ethylene group of methacryloyl group, the CH proton bonded to the NH group of amino acid, the –CH<sub>2</sub>– protons for cysteine and the –CH<sub>3</sub> group on methacryloyl moiety, respectively. <sup>13</sup>C (125 MHz, D<sub>2</sub>O), δ: 177.5, 172.9, 141.8, 122.6, 55.1, 30.1, 17.49 ppm.

The <sup>1</sup>H NMR and <sup>13</sup>C NMR peaks at 7.3 (d, 2H), 7.0 (d, 2H), 6.3 (s, 1H) were proved that MATyr monomer was synthesized. <sup>13</sup>C (125 MHz, DMSO-d<sub>6</sub>), δ: 170.9, 165.8, 149.6, 135.9, 130.9, 128.0, 121.8, 115.6, 55.9, 37.0, 18.5 ppm.

The elemental analysis results for Dichloro bis pyridyl ruthenium (II) (Ru(bipy)<sub>2</sub>Cl<sub>2</sub>) [C<sub>20</sub>H<sub>15</sub>Cl<sub>2</sub>N<sub>4</sub>Ru] was found as C 48.2%, H 3.0%, N 12.9%, calculated as C 49.7%, H 3.1%, N 11.6%. The <sup>1</sup>H NMR peaks at 10.2 ppm (d, 2H), 9.9 ppm (d, 2H), 9.7 ppm (d, 2H), 9.6 ppm (d, 2H) indicates that dichloro bis pyridyl ruthenium (II) (Ru(bipy)<sub>2</sub>Cl<sub>2</sub>) was synthesized. The MALDI-TOF-MS ion peaks at 413, 448 and 484 m/z were assigned to Ru(bipy)<sub>2</sub>, Ru(bipy)<sub>2</sub>Cl and Ru(bipy)<sub>2</sub>Cl<sub>2</sub>, respectively (Fig. 1). With the aid of the elemental analysis, MS spectra and <sup>1</sup>H NMR spectra, it has been proved that the dichloro bis pyridyl ruthenium (II) (Ru(bipy)<sub>2</sub>Cl<sub>2</sub>) molecule is synthesized exactly.

The elemental analysis results for Ru(bipy)<sub>2</sub>MATyrCl [C<sub>34</sub>H<sub>33</sub>ClN<sub>5</sub>O<sub>4</sub>Ru] was found as C 56.7%, H 5.0%, N 10.2%, calculated as C 57.3%, H 4.7%, N 9.8%. The <sup>1</sup>H NMR peaks at 9.7 ppm (d, 4H), 8.6 ppm (d, 4H), 7.9 ppm (t, 4H), 7.3 ppm (t, 1H), 7.2 ppm (t, 2H), 7.2 ppm (d, 2H), 7.1 ppm (t, 4H), 5.3 ppm (d, 1H), 5.3 ppm (d, 1H),

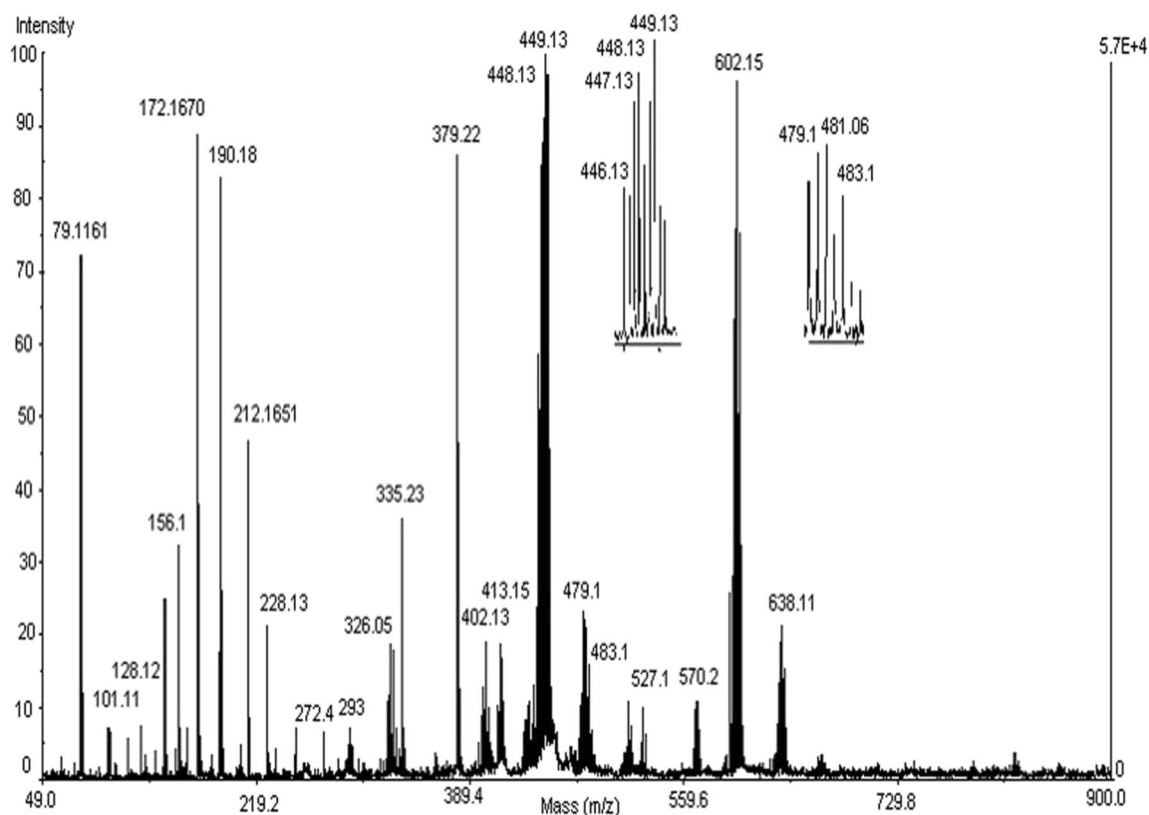
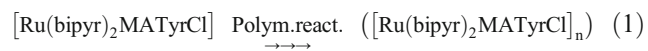


**Fig. 1** Matrix assisted time of flight mass spectrum of Dichloro bis pyridyl ruthenium (II) [Ru(bpy)<sub>2</sub>Cl<sub>2</sub>]. Instrument setting: 2  $\mu$ L of Ru(bpy)<sub>2</sub>Cl<sub>2</sub> solution was mixed with 23  $\mu$ L of 10 mgmL<sup>-1</sup> solution of  $\alpha$ -cyano-4-hydroxycinnamic acid (CHCA) in acetonitrile/0.3%

trifluoroacetic acid (TFA). The acceleration voltage was set to 20 kV, the delay time was 100 ns, grid voltage 65%, laser intensity 2200 and at reflector mode

1.8 ppm (s, 3H) proves that MATyr-Ru(bipyridyl)<sub>2</sub>Cl was synthesized. MATyr monomer and Ru-MATyr related ion peaks were obtained at 250 and 351 m/z, respectively. The obtained MS and NMR spectra and the data of elemental analyses confirmed that the synthesis of the Ru(bipyridyl)<sub>2</sub>MATyrCl was successfully achieved.

The photosensitive oligomer includes the repeating unit produced from ruthenium-based functional monomers and can be represented by the following Reaction 1. The photosensitive oligomer of Reaction 1 can be prepared by a conventional polymerization reaction. The polymer contains about 24 repeating units according to MALDI-TOF MS analyses (Fig. 2).



MATyr monomer, Ru-MATyr, Ru(bipyridyl)MATyrCl and Ru(bipyridyl)<sub>2</sub>MATyr related ion peaks have obtained at 250, 351, 541 and 662 m/z, respectively. The ion peaks at 413 and 448 m/z are belonged to Ru(bipyridyl)<sub>2</sub> and Ru(bipyridyl)<sub>2</sub>Cl, respectively.

### Measurement of Binding Interactions of Immunoglobulin M with Concanavalin a and Anti-IgM Decorated Quantum Dots

The binding ability of IgM with con A and anti-IgM decorated QD based nanocrystal was evaluated by using fluorescence spectroscopy. The fluorescence intensity of QDs functionalized with MACys which has hydrophilic thiol group has increased. When the second functionalization was carried out with MATyr monomer, fluorescence intensities of QDs also increased. On the other hand, the fluorescence intensity decreased when QDs were cross-linked and decorated with con A and anti-IgM solution in the presence of photosensitive ruthenium-based co-monomer. The obtained results showed that quenching occurs because of fluorescence resonance energy transfer (FRET) (Fig. 3.) FRET is an energy transfer method and this energy transfer occurs between the excited state of the donor to ground state of the acceptor by dipole-dipole interaction. Energy transfer efficiency depends on the distance (approximately 10–100 Å) from the donor to the acceptor. FRET has widely used the investigation of the protein-protein interactions, antibody-antigen interactions,

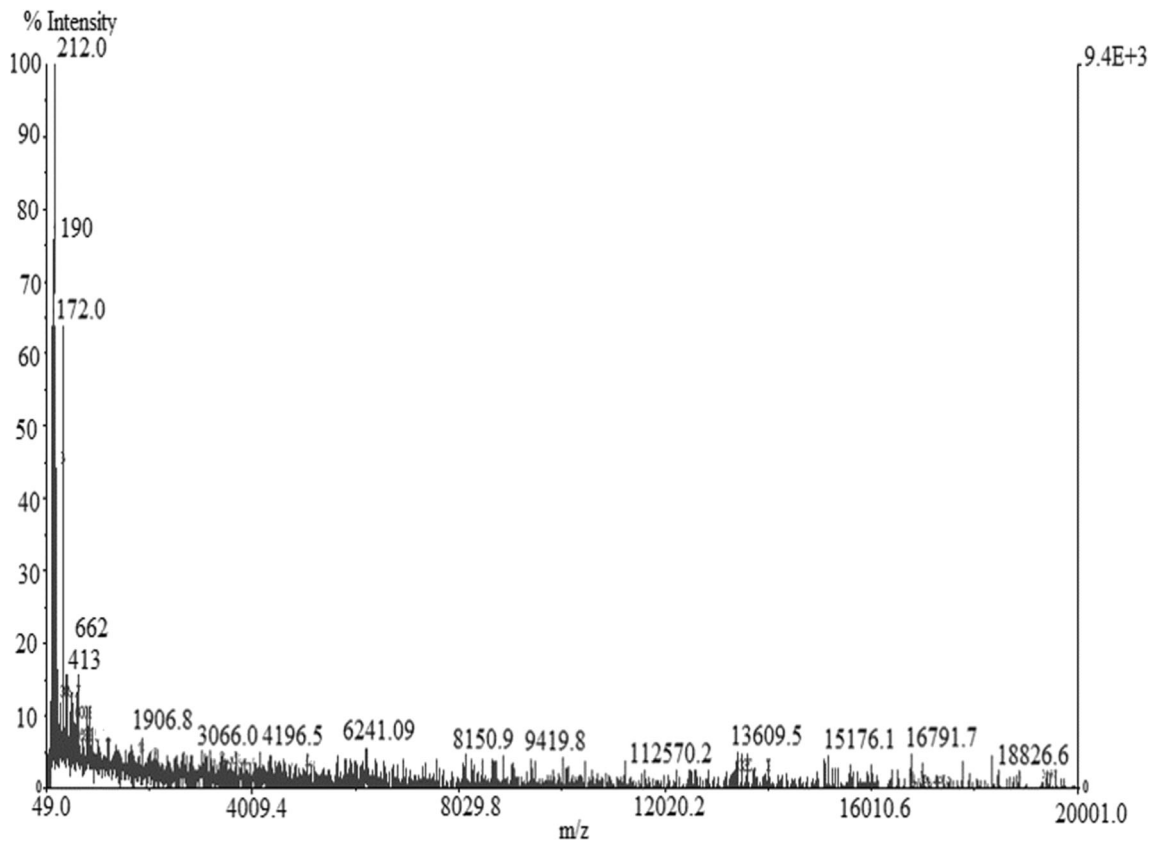
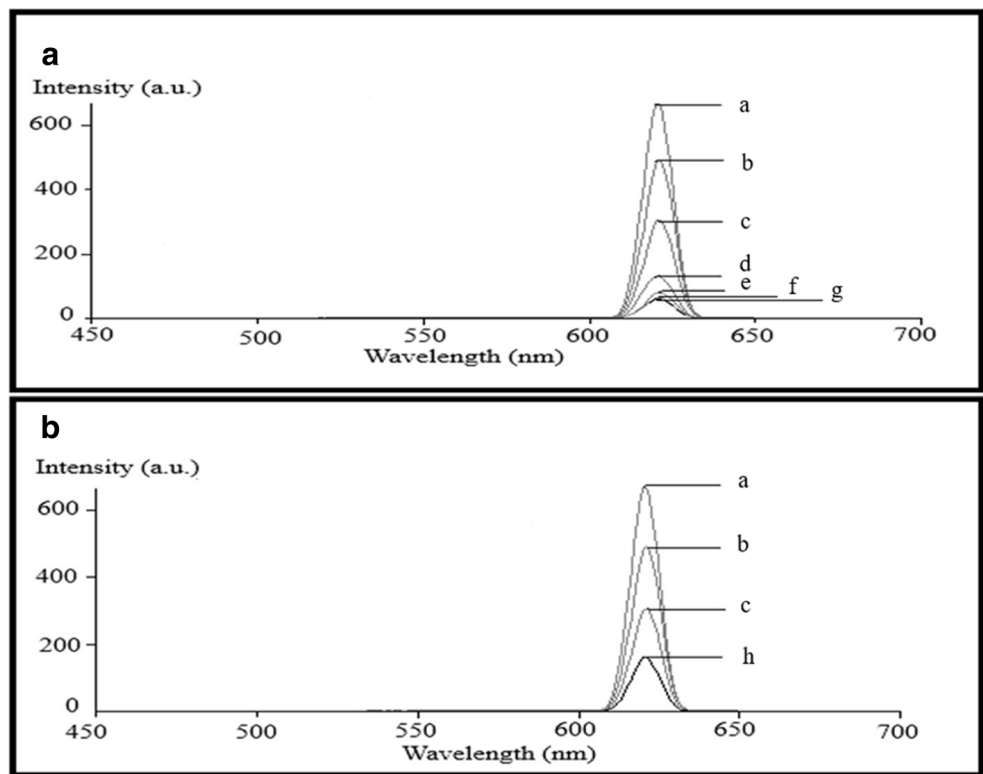


**Fig. 2** Matrix assisted time of flight mass spectrum of photosensitive ruthenium based polymers [P(Ru(bpy)<sub>2</sub>MATyrCl)]. Instrument setting: 1  $\mu$ L of P(MATyr-Ru(bpy)<sub>2</sub>-Cl) solution was mixed with 24  $\mu$ L of 10 mgmL<sup>-1</sup> solution of  $\alpha$ -cyano-4-hydroxycinnamic acid (CHCA) in

acetonitrile/0.3% trifluoroacetic acid (TFA). The acceleration voltage was set to 20 kV, the delay time was 100 ns, grid voltage 65%, laser intensity 2200 and at reflector mode

**Fig. 3** Fluorescence intensities of **a.** Fluorescence Intensities of Con A conjugated QD **b.** Fluorescence Intensities of anti IgM conjugated QD (MACys: methacryloylamido cysteine, MATyr: methacryloylamido tyrosine, Con A: Concanavalin A, IgM: Immunoglobulin M, a: MATyr Functionalized QD, b: MACys functionalized QD, c: QD, d: Con A conjugated QD, e: interaction of Con A conjugated QD and 1 ppm IgM, f: interaction of Con A conjugated QD and 0.5 ppm IgM, g: interaction of Con A conjugated QD and 0.01 ppm IgM, h: Anti IgM conjugated QD)



DNA-protein interactions, conformational change, DNA hybridization, and nanosensors studies [29–33]. The fluorescence intensities of the nanocrystals are given in Fig. 3.

When Con A and anti-IgM decorated QDs interacted with IgM, fluorescence intensities of QDs decreased due to binding. The fluorescence intensities of Con A and anti-IgM decorated QDs increased in proportional to IgM concentration.

Scatchard analysis [28, 34, 35] and Langmuir isotherm [28, 36] can be used for characterization of interaction. The affinity constants define the binding affinity between two molecules at equilibrium. The binding equation is as follows:



Where QDs and IgM-QDs represent Con A and anti-IgM decorated QDs and binding of IgM to QD nanocrystals. The interactions of anti-IgM and Con A decorated QD nanocrystals with IgM was given in Fig. 4.

Langmuir isotherm validation can be investigated by calculating the affinity constant using fluorescence intensities at equilibrium with various concentrations. The Langmuir

relationship can be determined by using Eq. 3:

$$C_0/I = 1/I_{\max} b + C_0/I_{\max} \quad (3)$$

Where  $C_0$ ,  $b$ , and  $I_{\max}$  are IgM concentration, Langmuir constant, and the maximum fluorescence intensity, respectively. The results obtained from the linearized form of the Langmuir isotherm were given in Table 1. The binding affinities of Con A and anti-IgM conjugated QDs,  $K_a$  and  $I_{\max}$  values were determined.

As seen from Table 1, in general value of  $K_a$  based on Langmuir analysis shows the accessibility of IgM molecules to all of the nanocrystals. Affinity constants for Con A and anti-IgM conjugated QDs were found to be  $42.75 \times 10^9 \text{ M}^{-1}$  and  $32.1 \times 10^9 \text{ M}^{-1}$ , respectively. Disassociation constant ( $K_D$ ) for Con A and anti-IgM conjugated QDs were obtained at 23.4 pM and 31.15 pM, respectively. Because of Con A has multiple binding sites for IgM binding, the affinity constant of ConA is higher than the affinity constant of anti-IgM. Con A is smaller than anti-IgM and also steric hindrances of Con A is less than anti-IgM. It is found that Con A decorated QDs has a more binding capacity for IgM. Youan et al. immobilized concanavalin A on QCM surface by using carbodiimide crosslinking and investigated binding analysis between

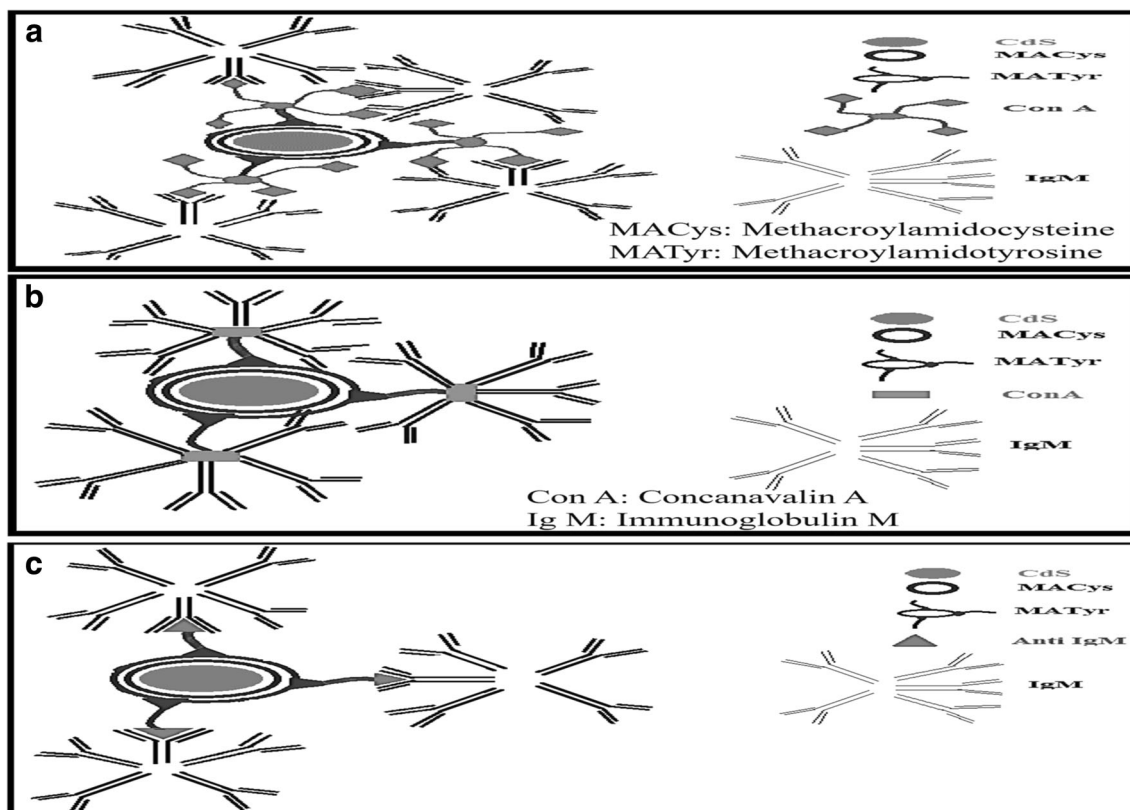


**Fig. 4** The schematic representation of interaction of Immunoglobulin M with a. Concanavalin A conjugated Quantum Dots b. Anti Immunoglobulin M conjugated Quantum Dots (MACys: methacroylamido cysteine, MATyr: methacroylamido tyrosine, Con A: Concanavalin A, IgM: Immunoglobulin M)

methacroylamido cysteine, MATyr: methacroylamido tyrosine, Con A: Concanavalin A, IgM: Immunoglobulin M)

**Table 1** Comparison of Langmuir analysis for Concanavalin A and anti Immunoglobulin M Conjugated Quantum Dots

|                        | Langmuir $K_a$ ( $M^{-1}$ ) | $I_{max}$ (a.u.) | $R^2$  |
|------------------------|-----------------------------|------------------|--------|
| Con A Conjugated QD    | $42.75 \cdot 10^9$          | 74.074           | 0.9915 |
| Anti-IgM Conjugated QD | $32.1 \cdot 10^9$           | 74.074           | 0.9905 |

ConA and mannan. The association constants were found to be as  $3.93 \cdot 10^6 M^{-1}$  and  $3.46 \cdot 10^5 M^{-1}$  for ConA-glycogen and Con A-mannan interactions by Youan et al., respectively.  $K_D$  values were calculated as  $0.25 \mu M$  and  $2.89 \mu M$ , respectively [37]. Mislovica et al. found the dissociation constants of mannan and its conjugates with BSA on Con A bead cellulose sorbent to be about  $2.81 \cdot 10^{-7}$  and  $8.98 \cdot 10^{-8} M$ . Mannan-BSA conjugates interaction with Con A was also investigated by SPR and found to be about  $5.32 \cdot 10^{-7}$  and  $3.25 \cdot 10^{-7} M$  [38]. Brewer et al. reported that Con A binds to tetravalent trimannoside analog was nearly four times greater than that of the corresponding monovalent analog mannose [39]. The results of obtained from Langmuir analysis showed that prepared proteinous polymeric shell decorated nanocrystals have a high affinity to IgM. It confirms that presented proteinous polymeric shell decorated nanocrystals are a robust platform for characterizing protein-ligand affinity.

The Langmuir adsorption isotherm presumes that the molecules are bound at a certain number of well-defined sites and this binding site is able of holding only one molecule [25]. These binding sites are also presumed to be energetically equivalent, homogeneous, and far away from each other in order not to disturb the interaction between the binding molecules. The fact that the correlation constant ( $R^2$ ) obtained from the Langmuir isotherm is close to the value of one indicates that the nanobioconjugation system is in favor of the Langmuir adsorption model. This adsorption model indicates that the binding site of nanocrystals is an energetically equivalent, homogeneous and distant from each other. By using ANADOLUCA method, orientated immobilization of proteins was carried out effectively.

The prepared proteinous polymeric shell decorated nanocrystals are of great potential in fundamental research as well as in applications in life sciences. Recently, Suda prepared [40] sugar chain immobilized fluorescent nanoparticles (SFNPs) as a point of care diagnostic application for Guillain-Barré Syndrome. Since SFNPs creates fluorescent aggregates with anti-ganglioside antibodies in sera with GBS, they were used successfully for visual detection under UV light. Bonsignori and Moody developed [41] simultaneous detection of specific IgG and IgM antibody-secreting cells by replacing the fluorophores with ODs. Matsui et al. [42] immobilized anti-human IgG and anti-mouse IgG antibodies simultaneously to coated nanotubes and they proved that the biological molecular

recognition between the multiple-antibody nanotubes and the complementary antigen arrays organized these antibody nanotubes according to the ordered arrays. Their approach was to immobilize antibody-coated nanotubes at particular complementary binding positions on surfaces.

## Conclusions

In this study, a novel protein immobilization approach which contains ruthenium-based functional monomer was developed. Immobilization of Con A and anti-IgM in the presence of photosensitive ruthenium-based functional monomers is an important step and orientated immobilization can be done in one step. This conjugation method, which is based on covalent and cross-linking, provides an appropriate antibody orientation by preventing denaturation of the antibody during the binding process. The photosensitive ruthenium-based functional monomers can efficiently be conjugated to various micro and nano-surfaces through chemical binding. Affinity constants for Con A and anti-IgM conjugated QDs were found to be  $42.75 \cdot 10^9 M^{-1}$  and  $32.1 \cdot 10^9 M^{-1}$ , respectively. Con A affinity to IgM was found to be quite as good as an anti-IgM antibody affinity to IgM. These results were shown the connections for investigation of lectin-antibody interactions. Prepared nanocrystals were also used in the determination of IgM. These nanocrystals are potential candidate substances for the determination of IgM in aqueous environments. QDs could be used for a wide range of biological studies by taking advantage of their fluorescent properties. IgM plays a central role in the initial response of the immune system to foreign antigens. An important approach to the rapid diagnosis of infectious diseases is the detection of specific IgM antibodies. IgM content in human serum can be used to estimate immune function and is an important parameter for diagnosing acute and chronic hepatitis, rheumatoid arthritis, hepatocirrhosis, malaria, typhoid, HIV infections, dengue fever, Waldeström macroglobulinemia, and malignant plasma cell tumors. Thus, a sensitive estimate of IgM is important in clinical laboratories. This prepared proteinous polymeric shell decorated nanocrystals are of great potential in fundamental research as well as in applications in life sciences and can be used in infection case studies or allergy symptoms.

## Compliance with Ethical Standards

**Conflict of Interest** The authors declare that there is no conflict of interest regarding the publication of this manuscript.

**Financial Interests** The authors declare no competing financial interest.

## References

- Tarköy M, Wyss M, Rudolf MP (2010) A comparative characterization of dipentameric (IgM)<sub>2</sub> and pentameric IgM species present in preparations of a monoclonal IgM for therapeutic use. *J Pharm Biomed Anal* 51:1084–1090. <https://doi.org/10.1016/j.jpba.2009.11.003>
- Evans SV, MacKenzie CR (1999) Characterization of protein-glycolipid recognition at the membrane bilayer. *J Mol Recognit* 12:155–168. [https://doi.org/10.1002/\(SICI\)1099-1352\(199905/06\)12:3<155::AID-JMR456>3.0.CO;2-S](https://doi.org/10.1002/(SICI)1099-1352(199905/06)12:3<155::AID-JMR456>3.0.CO;2-S)
- Patil S, Martinez NF, Lozano JR, Garcia R (2007) Force microscopy imaging of individual protein molecules with sub-pico Newton force sensitivity. *J Mol Recognit* 20:516–523. <https://doi.org/10.1002/jmr.848>
- Shepherd D (2005) *Encyclopedic reference of Immunotoxicology*. Springer-Verlag, Berlin, Heidelberg. <https://doi.org/10.1007/3-540-27806-0>
- Burrell CJ, Howard CR, Murphy FA (2017) Adaptive immune responses to infection. In: Fenner and White's *Medical Virology*. Elsevier, pp 65–76. <https://doi.org/10.1016/B978-0-12-375156-0.00006-0>
- Actor JK (2014) The B lymphocyte and the humoral response. In: *Introductory Immunology*. Elsevier, pp 28–41. <https://doi.org/10.1016/B978-0-12-420030-2.00003-2>
- Koppel R, Solomon B (2001) IgM detection via selective recognition by mannose-binding protein. *J Biochem Biophys Methods* 49:641–647. [https://doi.org/10.1016/S0165-022X\(01\)00225-1](https://doi.org/10.1016/S0165-022X(01)00225-1)
- Chen PJ, Wang JT, Hwang LH, Yang YH, Hsieh CL, Kao JH, Sheu JC, Lai MY, Wang TH, Chenet DS (1992) Transient immunoglobulin M antibody response to hepatitis C virus capsid antigen in posttransfusion hepatitis C: putative serological marker for acute viral infection. *Proc Natl Acad Sci U S A* 89:5971–5975
- Zhou JW, Lei LM, Liang QN, Liu TC, Lin GF, Dong ZN, Liang RL, Chen ZH, Wu YS (2015) Dual-labeled time-resolved immunofluorometric assay for the determination of IgM antibodies to rubella virus and cytomegalovirus in human serum. *Clin Biochem* 48:603–608. <https://doi.org/10.1016/j.clinbiochem.2015.01.009>
- Atias D, Liebes Y, Chalifa-Caspi V, Breman L, Lobel L, Marks RS, Dussart P (2009) Chemiluminescent optical fiber immunosensor for the detection of IgM antibody to dengue virus in humans. *Sensors Actuators B* 140:206–215. <https://doi.org/10.1016/j.snb.2009.03.044>
- Omar NAS, Fen YW (2017) Recent development of SPR spectroscopy as potential method for diagnosis of dengue virus E-protein. *Sens Rev* 38:106–116. <https://doi.org/10.1108/SR-07-2017-0130>
- Darwish NT, Alias YB, Khor SM (2015) An introduction to dengue-disease diagnostics. *TrAC Trends Anal Chem* 67:45–55. <https://doi.org/10.1016/j.trac.2015.01.005>
- de Swart RL, Vos HW, UytdeHaag FG et al (1998) Measles virus fusion protein- and hemagglutinin-transfected cell lines are a sensitive tool for the detection of specific antibodies by a FACS-measured immunofluorescence assay. *J Virol Methods* 71:35–44. [https://doi.org/10.1016/S0166-0934\(97\)00188-2](https://doi.org/10.1016/S0166-0934(97)00188-2)
- Jiang Z, Wei L, Zou M et al (2008) Rapid assay of trace immunoglobulin M by a new immunonanolod resonance scattering spectral probe. *J Biomol Screen* 13:302–308. <https://doi.org/10.1177/1087057108316737>
- Diltemiz SE, Ersöz A, Hür D, Keçili R, Say R (2013) 4-Aminophenyl boronic acid modified gold platforms for influenza diagnosis. *Mater Sci Eng C* 33:824–830. <https://doi.org/10.1016/j.msec.2012.11.007>
- Zheng H, Du X (2009) Enhanced binding and biosensing of carbohydrate-functionalized monolayers to target proteins by surface molecular imprinting. *J Phys Chem B* 113:11330–11337. <https://doi.org/10.1021/jp9060279>
- Boschetti E, Jungbauer A (2000) Separation of antibodies by liquid chromatography. *Sep Sci Technol* 2:535–632. [https://doi.org/10.1016/S0149-6395\(00\)80062-8](https://doi.org/10.1016/S0149-6395(00)80062-8)
- Chen GY, Chen CY, Chang MDT, Matsuura Y, Hu YC (2009) Concanavalin a affinity chromatography for efficient baculovirus purification. *Biotechnol Prog* 25:1669–1677. <https://doi.org/10.1002/btpr.253>
- Bronzoni RVM, Fatima M, Montassier S, Pereira GT, Gama NMSQ, Sakai V, Montassier HJ (2005) Detection of infectious bronchitis virus and specific anti-viral antibodies using a concanavalin A-Sandwich-ELISA. *Viral Immunol* 18:569–578. <https://doi.org/10.1089/vim.2005.18.569>
- Swierczewska M, Liu G, Lee S, Chen X (2012) High-sensitivity luminescent nanosensors for biomarker detection. *Chem Soc Rev* 41:2641–2655. <https://doi.org/10.1039/C1CS15238F>
- Rizvi S, Ghaderi S, Keshtgar M, Seifalian A (2010) Semiconductor quantum dots as fluorescent probes for in vitro and in vivo biomolecular and cellular imaging. *Nano Rev* 1:1–15. <https://doi.org/10.3402/nano.v1i0.5161>
- Costa-Fernández JM, Pereiro R, Sanz-Medel A (2006) The use of luminescent quantum dots for optical sensing. *TrAC Trends Anal Chem* 25:207–218. <https://doi.org/10.1016/j.trac.2005.07.008>
- Bilan R, Fleury F, Nabiev I, Sukhanova A (2015) Quantum dot surface chemistry and functionalization for cell targeting and imaging. *Bioconjug Chem* 26:609–624. <https://doi.org/10.1021/acs.bioconjchem.5b00069>
- Rusmini F, Zhong Z, Feijen J (2007) Protein immobilization strategies for protein biochips. *Biomacromolecules* 8:1775–1789. <https://doi.org/10.1021/bm061197b>
- Say R, Büyüktiryaki S, Hür D, Yılmaz F, Ersöz A (2012) Mutual recognition of TNT using antibodies polymeric shell having CdS. *Talanta* 90:103–108. <https://doi.org/10.1016/j.talanta.2012.01.007>
- Say R. (2011) Photosensitive Aminoacid-Monomer Linkage and Bioconjugation Applications in Life Sciences and Biotechnology. U.S. Patent No 20110311505 A1, World Intellectual Property Organization-PatentScope. Available at: [www.wipo.int/patentscope/search/en/WO2011070402](http://www.wipo.int/patentscope/search/en/WO2011070402). (Pub. No.: WO/2011/070402; Int. Appl. No.: PCT/IB2009.055707)
- Hur D, Ekti SF, Say R (2007) N-acylbenzotriazole mediated synthesis of some methacrylamido amino acids. *Lett Org Chem* 4:585–587. <https://doi.org/10.2174/157017807782795556>
- Diltemiz SE, Say R, Büyüktiryaki S, Hür D, Denizli A, Ersöz A (2008) Quantum dot nanocrystals having guanosine imprinted nanoshell for DNA recognition. *Talanta* 75:890–896. <https://doi.org/10.1016/j.talanta.2007.12.036>
- Mattoussi H, Medintz IL, Clapp AR, Goldman ER, Jaiswal JK, Simon SM, Mauro JM (2004) Luminescent quantum dot-bioconjugates in immunoassays, FRET, biosensing, and imaging applications. *J Lab Autom* 9:28–32. <https://doi.org/10.1016/S1535-5535-03-00083-2>
- Stringer RC, Schommer S, Hoehn D, Grant SA (2008) Development of an optical biosensor using gold nanoparticles and quantum dots for the detection of porcine reproductive and respiratory syndrome virus. *Sensors Actuators B Chem* 134:427–431. <https://doi.org/10.1016/j.snb.2008.05.018>
- Jamieson T, Bakhshi R, Petrova D, Pocock R, Imani M, Seifalian AM (2007) Biological applications of quantum dots. *Biomaterials* 28:4717–4732. <https://doi.org/10.1016/j.biomaterials.2007.07.014>
- Xu C, Xing B, Rao J (2006) A self-assembled quantum dot probe for detecting -lactamase activity. *Biochem Biophys Res Commun* 344:931–935. <https://doi.org/10.1016/j.bbrc.2006.03.225>
- Smith AM, Duan H, Mohs AM, Nie S (2008) Bioconjugated quantum dots for in vivo molecular and cellular imaging. *Adv Drug*

- Deliv Rev 60:1226–1240. <https://doi.org/10.1016/j.addr.2008.03.015>
34. Tsoi PY, Yang J, Sun Y, Sui SF, Yang M (2000) Surface Plasmon resonance study of DNA polymerases binding to template/primer DNA duplexes immobilized on supported lipid monolayer. *Langmuir* 16:6590–6596. <https://doi.org/10.1021/la9912951>
35. Yang M, Tsoi PY, Li CW, Zhao J (2006) Analysis of interactions of template/primer duplexes with T7 DNA polymerase by oligonucleotide microarray. *Sensors Actuators B Chem* 115:428–433. <https://doi.org/10.1016/j.snb.2005.10.008>
36. Persson B, Stenhag K, Nilsson P, Larsson A, Uhlén M, Nygren P (1997) Analysis of oligonucleotide probe affinities using surface plasmon resonance: a means for mutational scanning. *Anal Biochem* 246:34–44. <https://doi.org/10.1006/abio.1996.9988>
37. Coulibaly FS, Youan B-BC (2014) Concanavalin a–polysaccharides binding affinity analysis using a quartz crystal microbalance. *Biosens Bioelectron* 59:404–411. <https://doi.org/10.1016/j.bios.2014.03.040>
38. Mislovičová D, Masárová J, Švitel J et al (2002) Neoglycoconjugates of mannan with bovine serum albumin and their interaction with lectin concanavalin a. *Bioconjug Chem* 13:136–142. <https://doi.org/10.1021/bc015517u>
39. Dam TK, Roy R, Das SK, Oscarson S, Brewer CF (2000) Binding of multivalent carbohydrates to concanavalin A and *Dioclea grandiflora* lectin. Thermodynamic analysis of the “multivalency effect”. *J Biol Chem* 275:14223–14230. <https://doi.org/10.1074/jbc.275.19.14223>

**Publisher’s Note** Springer Nature remains neutral with regard to jurisdictional claims in published maps and institutional affiliations.